Inorganic Chemistry

ARTICLE

pubs.acs.org/IC

Behavior of Ag_3 Clusters Inside a Nanometer-Sized Space of ZSM-5 Zeolite

Takashi Yumura,*[,†] Tomohiro Nanba,[†] Hiroe Torigoe,[‡] Yasushige Kuroda,[‡] and Hisayoshi Kobayashi[†]

[†]Department of Chemistry and Materials Technology, Kyoto Institute of Technology, Matsugasaki, Sakyo-ku, Kyoto, 606-8585, Japan

[‡]Department of Fundamental Material Science, Division of Molecular and Material Science, Graduate School of Natural Science and Technology, Okayama University, Tsushima, Kita-ku, Okayama 700-8530, Japan

Supporting Information

ABSTRACT: We found from DFT calculations that Ag−Ag orbital interactions as well as Ag−O electrostatic interactions determine the structures of three silver cations inside a nanometer-sized cavity of ZSM-5 (Ag_3−ZSM-5) in lower and higher spin states. Both interactions strongly depend on the number of Al atoms substituted for Si atoms on the ZSM-5 framework (ZSM-5(Al_n)), where n ranges from 1 to 3. In smaller n, stronger Ag−Ag orbital interactions and weaker Ag−O electrostatic interactions operate. Accordingly, there are significant dependencies of the structures of three silver cations on the number of Al atoms. In lower spin states of Ag_3−ZSM-5(Al_1) and Ag_3−ZSM-5(Al_2), D_{3h}-like triangle clusters are contained inside ZSM-5 whereas their higher spin states have triangle clusters distorted significantly from the D_{3h} structure. In lower spin states, the totally symmetric orbital consisting of 5s(Ag) orbitals is responsible for cluster formation, whereas in higher spin states occupation of a 5s(Ag)-based orbital with one node results in significant distortion of the triangle clusters. The distortion can be partially understood by analogies to Jahn−Teller distortion of the bare D_{3h} Ag_3^+ cluster in the triplet spin state. When n is 3, we found that three silver cations are isolated in a lower spin state and that a linear cluster consisting of two silver cations is formed in a higher spin state. Thus, we demonstrate from DFT calculations that the number of Al atoms can control the properties of three silver cations inside a ZSM-5 cavity. Since the structural and electronic features of the enclosed silver clusters can link to their catalytic properties, the DFT findings can help us to understand the catalytic activity of Ag−ZSM-5.

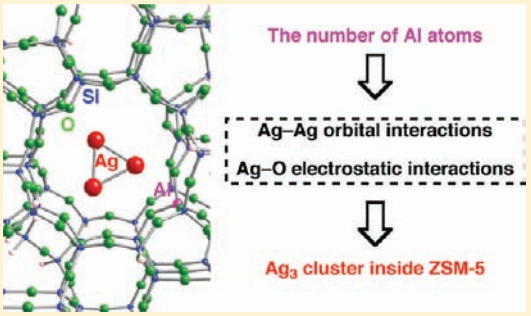

INTRODUCTION

Zeolites,[1−4] aluminosilicate-based porous materials, serve as nanocontainers because they can incorporate various guest species,[5,6] similar to carbon nanotubes.[7−10] Encapsulation of guests in a restricted environment of a host (zeolite[11] and nanotube[12]) would change the properties of guests. Through host−guest interactions, even unstable species are stabilized to exist inside a nanometer-size cavity of a host.[12] In zeolite−guest interactions, substituting Al^{3+} for Si^{4+} on SiO_2 frameworks plays an essential role, because the substitution bears negative charges on framework oxygen atoms neighboring the Al sites. By the requirements of charge balance, various cations are bound in the vicinity of the substitution sites. Then, the negatively charged oxygen atoms can have an influence on the structures of guest species. Sometimes the inner cations aggregate to form unusual small cation clusters, because they are stabilized by interactions with negatively charged oxygen atoms of zeolites.

For example, small silver clusters consisting of 2−8 atoms have been reported to exist inside zeolite cavities.[13−26] Depending on the size of enclosed silver species, silver-containing zeolites exhibit quite unique optoelectronic properties.[26] The size dependences are owing to quantum-size effects of small clusters, because they have discrete energy levels that are generated by quantization of the wavevector in its bulk.[27] Beside the unique electronic properties, smaller silver clusters inside zeolites exhibit catalytic activity. The catalytic properties would also depend strongly on the number of silver atoms in active species, similar to nanometer-size gold catalysts.[28] Thus, many researchers have been making an intense effort to elucidate how many atoms are really contained in the active silver clusters. In terms of the catalytic activity, the existence of coordinatively unsaturated metal atoms in clusters is additionally indispensable. Despite their intriguing properties, we cannot fully understand structures of silver clusters embedded inside a zeolite cavity as well as how their structures link to the properties.

In the present study, we focus on the structural features of silver clusters inside a nanometer-size cavity of ZSM-5. Experimentally Ag−ZSM-5 allows one to catalyze NOx decomposition[20−22] as well as activate a C−H bond of hydrocarbons.[23−25] With respect to the catalytic reactions in ZSM-5, many experimental reports suggest that silver clusters

Received: January 22, 2011
Published: June 21, 2011

with nuclearity smaller than 4 are formed as active species. For example, Satsuma et al. found that Ag−ZSM-5 reduces NO to N_2 in the presence of hydrocarbons, and the reaction is promoted by a small amount of H_2.[22] To clarify the size of silver clusters formed upon H_2 reduction, they measured UV−vis spectroscopy and found bands at 255 and 305 nm. On the basis of UV−vis measurements together with EXAFS analyses, they proposed that H_2 reduction of Ag−ZSM-5 produces inner Ag_4^{2+} clusters as the active sites. However, they cannot exclude formation of Ag_4^{3+}, Ag_2^{+}, and Ag_3^{2+} as possible active species. In fact, the UV−vis band positions are close to those observed in X and Y zeolites, where $Ag_3^{\delta+}$ clusters are proposed to be formed.[16]

Turning to activation of a C−H bond of hydrocarbons by Ag−ZSM-5,[23−25] ions or clusters (such as Ag_3^{+})[25] are responsible for the reactions. Interestingly, different reaction products were formed depending on pretreatment of silver-ion-exchanged ZSM-5s (oxidation as well as reduction by H_2 treatment or by photoirradiation).[24] In particular, photoreduced Ag−ZSM-5s transform CH_4 into C_2H_6 under photoirradiation, whereas H_2-reduced Ag−ZSM-5s can catalyze conversion of CH_4 into C_2H_4 by heat treatment.[24] The different reactivity between the two reduced Ag−ZSM-5s comes from the size of silver clusters as its active species; larger clusters were expected to be formed in H_2-reduced Ag−ZSM-5 relative to the photoreduced Ag−ZSM-5 cases. Note that similar catalytic reactions were also reported under photoirradiation of silver-containing zeolite Y, where enclosed Ag_3^{2+} clusters are expected to behave as the active site.[16] Photoirradiation would induce an electron to be excited from an occupied orbital of Ag−ZSM-5 to an unoccupied orbital.[29]

Although experimental papers proposed that the active sites inside a ZSM-5 cavity contain three or four silver ions, it is still desirable to shed light on the atomic configurations of enclosed Ag clusters in lower and higher spin states with the aid of computational chemistry. In this direction, we employed density functional theory (DFT) calculations to elucidate factors determining the structures of silver clusters inside a ZSM-5 cavity. Currently, DFT methods can provide helpful insight into structure−reactivity relationships in reactive metal guests inside a zeolite cavity.[30] Considering the various experimental reports and computational limitation, the present study focuses on an Ag_3 cluster inside a ZSM-5 zeolite to obtain basic information on the behavior of the enclosed silver clusters. In the DFT calculations, we will discuss how structures of the Ag_3 cluster are affected by the number of substituted Al atoms as well as different spin states.

METHOD OF CALCULATION

In previous studies,[31] we constructed an aluminum-free ZSM-5 model (silicalite-1) including a 10-membered ring (10-MR) cavity, as shown in Figure S1 (Supporting Information).[32] The silicalite-1 model has a $Si_{92}O_{151}$ framework whose terminal Si atoms are saturated by the H atoms ($Si_{92}O_{151}H_{66}$). To construct the Ag_3−ZSM-5 model, we put an Ag_3 cluster inside a 10-MR cavity of the $Si_{92}O_{151}H_{66}$ model and at the same time some Al atoms are substituted for Si atoms. In the present study, the number of substituted Al atoms (n) varies from 1 to 3. To represent $Ag_3-Al_nSi_{92-n}O_{151}H_{66}$, the notation of Ag_3−ZSM-5(Al_n) will be used throughout this paper. By using DFT methods, we fully optimized Ag_3−ZSM-5(Al_n) structures.

Searching DFT functionals suitable to describe properly the properties of silver clusters,[33−37] we tested the B3LYP,[38−40] B3PW91,[41] and PBEPBE[42] functionals by using bare Ag_3 clusters as a test case. Then these results were compared with that obtained from coupled cluster singlet double (CCSD)[43] calculations which are more reliable than DFT calculations. Detailed discussions of the optimized structures can be seen in the Supporting Information. Briefly, DFT calculations found two types of bare Ag_3 clusters (acute isosceles and obtuse isosceles triangles, as shown in Figure S2 and Table S1 (Supporting Information)), while CCSD calculations found only one local minimum, an acute isosceles triangle. In terms of whether DFT calculations can reproduce CCSD results, B3PW91 and PBEPBE functionals are more suitable than the B3LYP functional. Although the energy differences are up to 1 kcal/mol irrespective of functionals, we can differentiate B3LYP results from B3PW91 and PBEPBE results. The differences may come from the failure of the LYP functional in B3LYP calculations to describe silver clusters and its metals.[44] Accordingly, we used the B3PW91 functional to analyze the structures of Ag_3 species inside ZSM-5 in the following sections. However, B3LYP calculations have been prevalent among chemists, because they can reproduce well experimental data, in particular, geometries and vibrational frequencies. We also optimized Ag_3−ZSM-5(Al_n) geometries by using the B3LYP functional to check whether the structural features obtained from B3PW91 calculations can be reproduced. As a result of the calculations, we confirmed that the B3PW91 and B3LYP calculations basically yielded similar Ag−Ag and Ag−O bondings in Ag_3−ZSM-5(Al_n), as will be seen below. Although there are some theoretical works on silver-containing zeolites,[45−48] the present investigation is more appropriate to study effects of the ZSM-5 surroundings on the structures of silver clusters in terms of the accuracy of calculation methods as well as the size of the silver-containing zeolite model.

In the optimization using Gaussian03 code[49] and partially Gaussian09 code,[50] we used the CEP-121G basis set for extraframework Ag atoms,[51] the 6-31G basis set for substituted Al atoms, and two O atoms that are bound to a substituted Al atom[52] and the 3-21G basis set for the other atoms,[53] due to limitations of computational resources. Accordingly, the calculations of Ag_3−ZSM-5(Al_1), Ag_3−ZSM-5(Al_2), and Ag_3−ZSM-5(Al_3) involve 2795, 2810, and 2825 contracted basis functions. When the ZSM-5 model contains two substituted Al atoms, Ag_3−ZSM-5(Al_2) has odd-numbered electrons. Therefore, we considered its doublet state as a lower spin state and quartet state as a higher spin state. In the other cases (n = 1 and 3) where the Ag_3−ZSM-5(Al_n) models have even-numbered electrons, its lower (higher) spin states are spin singlet (triplet). Accordingly, unrestricted DFT calculations were used for optimization of Ag_3−ZSM-5, except for the singlet spin state of Ag_3−ZSM-5(Al_2) where we used restricted DFT calculations.

RESULTS AND DISCUSSION

Deformation of Bare Ag_3^{+} Clusters in Singlet and Triplet Spin States. Prior to discussing positively charged Ag_3 clusters inside a ZSM-5 cavity, we investigate the properties of Ag_3^{+} and Ag_3^{2+} clusters in the gas phase based on B3PW91 calculations. Their key parameters are listed in Table 1. The optimized Ag_3^{+} cluster has the D_{3h} structure with Ag−Ag separations of 2.721 Å (Table 1).[54] The separations are close to those obtained in Ag_3−ZSM-5(Al_1) and Ag_3−ZSM-5(Al_2), as will be seen below. On the other hand, the Ag_3^{2+} cluster optimized under

Table 1. Key Parameters of the Bare Ag_3^{+} and Ag_3^{2+} Clusters with D_{3h} Symmetry, Obtained from B3PW91 Calculations

cluster	Ag−Ag[a]	$\nu(E')$[b]	$\nu(A_1)$[b]	excitation energy[c]
Ag_3^{+}	2.721	115.4	169.7	318 (0.30)[d]
Ag_3^{2+}	3.126	37.3	67.5	327 (0.12)[d], 345 (0.09)[d]

[a] Ag−Ag (Å): Ag−Ag separations (Ag1−Ag2 = Ag2−Ag3 = Ag3−Ag1) are defined in Chart 1. [b] $\nu(E')$, $\nu(A_1)$ (cm^{-1}): calculated vibrational frequencies. Their modes can be seen in Chart 2. [c] Excitation energy (nm): Calculated excitation energy whose oscillation strength is relatively significant. [d] Calculated oscillation strength

dx.doi.org/10.1021/ic2001514 |Inorg. Chem. 2011, 50, 6533–6542

Chart 1

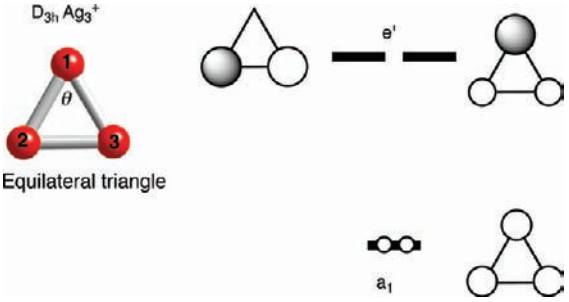

Chart 2

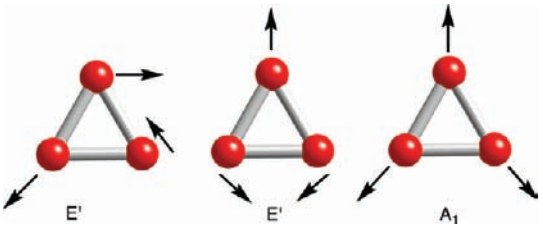

D_{3h} symmetry constraints has longer Ag−Ag separations of 3.126 Å.

Since the Ag_3^+ cluster has Ag−Ag separations similar to those in Ag_3−ZSM-5(Al_1) and Ag_3−ZSM-5(Al_2), we confine our attention to the electronic properties of the Ag_3^+ cluster. Dependences of the geometrical parameters on calculation methods (B3PW91, B3LYP, PBEPBE, and CCSD methods) can be seen in Table S2, Supporting Information. Considering the $[Kr](4d)^{10}(5s)^1$ configuration in the neutral silver atom, the singlet state of the D_{3h} Ag_3^+ cluster has the $(a_1)^2(e')^0$ configuration in Chart 1.[55] Its vibrational modes (one A_1 mode and two E′ modes) and their frequencies are seen in Chart 2 and Tables 1 and S2, Supporting Information, respectively. Also, we performed time-dependent (TD) DFT calculations to investigate how photoexcitation induces electron transfers from the ground state to an excited state. According to TDDFT calculations, a substantial oscillation strength ($f = 0.30$) is seen in the transition where one electron in the a_1 orbital moves to an e′ orbital. The calculated excitation energy in the bare Ag_3^+ cluster is 318 nm. Corresponding excitation energies in the bare Ag_3^{2+} cluster are 327 and 345 nm. Both calculated values are comparable to those obtained experimentally. A different perspective in the DFT results suggests that it is difficult to definitely distinguish between the Ag_3^+ and Ag_3^{2+} clusters by their excitation energies.

On the basis of TDDFT calculations, we assume that in a higher spin state an e′ orbital and the a_1 orbital are assumed to be singly occupied. The resultant electronic $(a_1)^1(e')^1$ configuration is spin triplet. Then the triplet Ag_3^+ structure would distort along a single E′ vibrational mode to be stabilized, following Jahn−Teller theory.[56] Detailed discussion on the Jahn−Teller distortion in the triplet state can be seen in the Supporting Information. Following the Jahn−Teller distortion, we look into changes of potential energies of the D_{3h} Ag_3^+ structure ($Q(D_{3h})$) distorted along a vibrational mode of E′ symmetry in Chart 2. The distorted Ag_3^+ clusters can be given by $Q(D_{3h}) + \Delta Q_{E'}$, where $Q_{E'}$ is a small displacement along a single E′ vibrational mode and

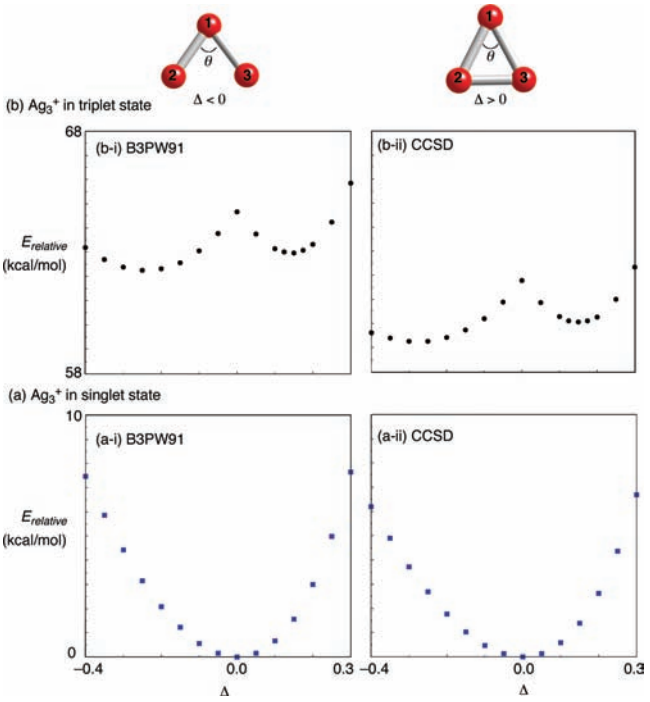

Figure 1. Potential energy surfaces in the singlet and triplet spin states of the Ag_3^+ cluster distorted along a single E′ vibration ($Q(D_{3h}) + \Delta Q_{E'}$), where Δ represents how distorted a cluster is from the D_{3h} structure ($Q(D_{3h})$) along the E′ vibration ($Q_{E'}$). Energies of the distorted Ag_3^+ clusters in the singlet (a) and triplet (b) states are given relative to the D_{3h} cluster in the singlet state ($E_{relative}$ in kcal/mol). The energy values were obtained from B3PW91 and CCSD calculations. Corresponding values obtained from B3LYP calculations can be seen in Figure S3 (Supporting Information). Key parameters of two stable conformations are given in Tables 2 and S3 (Supporting Information).

Δ (a nondimensional parameter) represents how distorted a cluster is from the D_{3h} structure along the vibration. Similar procedures have already been devised by Yoshizawa and coworkers to discuss the vibrational−electronic interactions in the mono- and trianions of benzene and [18]annulene.[57] Following Yoshizawa et al.,[57] we employed B3PW91 calculations to see the energy changes of distorted Ag_3^+ clusters ($Q(D_{3h}) + \Delta Q_{E'}$) in the singlet and triplet states, as displayed in Figure 1a and 1b, respectively. For comparison, corresponding values based on CCSD calculations are also displayed in Figure 1. Figure 1a shows that the total energy in the singlet Ag_3^+ cluster increases with an increase in the absolute value of Δ. This suggests that the D_{3h} structure in the singlet state is stable with respect to the distortion. On the other hand, in the triplet state (Figure 1b), the E′ vibrational mode in the D_{3h} Ag_3^+ cluster leads to two stable conformations (Table 2): one triangle with a positive Δ value has a triangle with ∠Ag2−Ag1−Ag3 (θ) ≈ 55, and the other triangle with a negative Δ value has a triangle with $\theta \approx 70$. As shown in Chart 3, two a_1 orbitals are occupied singly in a distorted triangle with $\theta < 60$, whereas one a_1 and one b_2 orbitals are occupied singly in a distorted triangle with $\theta > 60$. Accordingly, they have different spin density distributions in Table 2; in a distorted triangle with $\theta \approx 55$, one ion has significant spin densities, while spin densities are mainly distributed into two ions in a distorted triangle with $\theta \approx 70$. Figure 1 and Table 2 show that the energy difference between the two distorted triangles is only ∼0.7 kcal/mol at CCSD and B3PW91 calculations. Similar

dx.doi.org/10.1021/ic2001514 |Inorg. Chem. 2011, 50, 6533–6542

results can be reproduced by B3LYP and PBEPBE methods, as shown in Figure S3 and Table S3 (Supporting Information).

Table 2. Key Parameters of Stable Conformations of the Bare Ag_3^+ Cluster in the Triplet Spin State, Obtained from B3PW91 and CCSD Calculations[a]

	angle		bond lengths			spin density[e]			
method	Δ[b]	θ[c]	Ag1−Ag2[d]	Ag2−Ag3[d]	Ag3−Ag1[d]	Ag1	Ag2	Ag3	ΔE[f]
B3PW91	0.150	54.9	2.755	2.579	2.835	0.88	0.54	0.58	0.72
B3PW91	−0.250	69.0	2.682	2.959	2.540	0.49	0.78	0.72	0
CCSD	0.150	54.8	2.852	2.623	2.852	0.84	0.58	0.58	0.79
CCSD	−0.30	71.3	2.636	3.073	2.636	0.54	0.73	0.73	0

[a] Corresponding B3LYP and PBEPBE values can be seen in Table S3 (Supporting Information). [b] Δ represents how distorted a cluster is from the D_{3h} structure ($Q(D_{3h})$) along a single E′ vibrational mode. Here a distorted cluster is given by $Q(D_{3h}) + \Delta Q_{E'}$, where $Q_{E'}$ is a small displacement along a single E′ mode in Chart 2. [c] θ (degree): optimized angle of ∠Ag2−Ag1−Ag3 [d] Ag1−Ag2, Ag2−Ag3, Ag3−Ag1 (Å): Ag−Ag separations, defined in Figure 1. [e] Spin density; calculated spin density integrated over atomic basin of an atom. [f] ΔE (kcal/mol): energy of a triangle relative the most stable conformation. When a triangle is the most stable conformation, ΔE is 0.

Chart 3

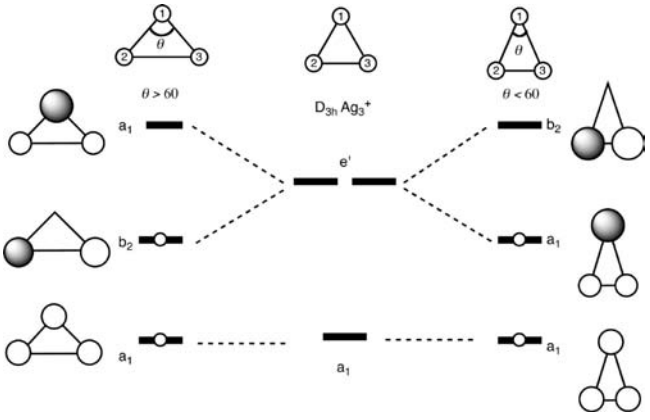

These analyses show that interactions between the 5s orbitals of silver ions are key in determining the structural and electronic properties of the bare Ag_3^+ clusters in the singlet and triplet spin states.

Behavior of an Ag_3 Cluster Inside a 10-MR of ZSM-5. Here, an important question arises as to how the properties of the Ag_3 cluster are influenced by its encapsulation into a 10-MR of ZSM-5. Inside a ZSM-5 cavity, interactions between a silver atom and a framework oxygen atom play an additional role in the structures of the enclosed Ag_3 clusters. In the Ag−O interactions, substitution of an Al atom for a Si atom is important because negatively charged oxygen atoms exert an electrostatic force on silver cations. Accordingly, the Ag−Ag orbital interactions as well as the Ag−O electrostatic interactions are expected to determine the structures of silver species inside a ZSM-5 cavity.

Properties of Ag_3−ZSM-5 in Lower Spin States. First, we would like to consider the behavior of an Ag_3 cluster inside a ZSM-5(Al_n) cavity with a focus on formal charges of clusters and zeolite frameworks. The ZSM5 framework with n-substituted Al atoms has $-n$ charge. Conversely, the formal charge of an Ag_3 cluster inside the ZSM-5 zeolite with n Al atoms is n. Considering Chart 1, the frontier occupied orbitals of an Ag_3 cluster inside ZSM-5(Al_n) in $n \leq 2$ would have 5s(Ag) character while that in $n = 3$ would have 4d(Ag) character. Since the frontier occupied orbitals of silver species contribute to determining their structural features inside a ZSM-5, their structures depend on n. Looking at the Ag−O interactions, negatively charged oxygen atoms of ZSM-5 emerged by substitution are important in the electrostatic interactions with a silver cation. In ZSM-5 framework with larger n, there would be larger numbers of negatively charged oxygen atoms. Accordingly, stronger electrostatic interactions would operate between three silver species and a ZSM-5 framework in this situation. Since the number of Al atoms would be responsible for both Ag−Ag and Ag−O interactions, the structures of silver species are expected to be susceptive to the Al substitution.

Taking the electron-count argument into account, we investigate B3PW91-optimized structures for lower spin states of Ag_3−ZSM-5(Al_n) whose local structures are given in Figure 2. In each Ag_3−ZSM-5(Al_n) configuration, we considered one possibility of Al position(s), due to limitations of computational resources. Corresponding B3LYP-optimized geometries are displayed in Figure S4 (Supporting Information). Detailed

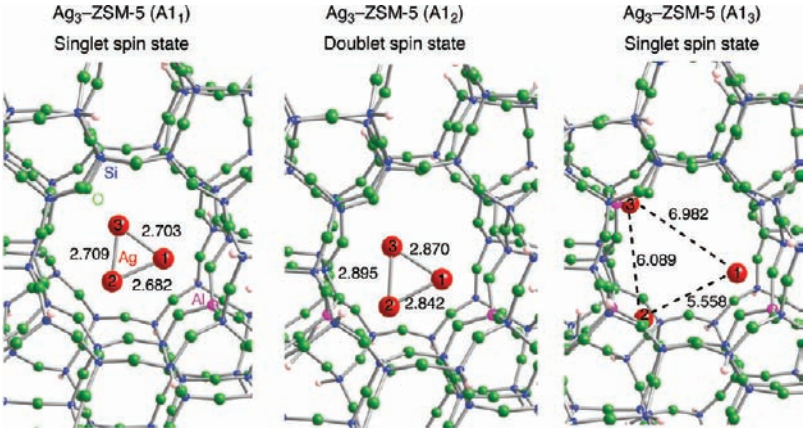

Figure 2. B3PW91-optimized Ag_3−ZSM-5(Al_n) structures in lower spin states where n varies from 1 to 3. Ag_3−ZSM-5(Al_1) and Ag_3−ZSM-5(Al_3) in the singlet spin state and Ag_3−ZSM-5(Al_2) in the doublet spin state are given. The Ag−Ag separations are given in Angstroms. Corresponding B3LYP-optimized geometries are given in Figure S4 (Supporting Information). Details of optimized Ag−O bond lengths can be seen in Tables 3 and S4 (Supporting Information).

dx.doi.org/10.1021/ic2001514 |Inorg. Chem. 2011, 50, 6533–6542

Table 3. Ag−O Bond Lengths of Ag_3−ZSM-5(Al_n) in Lower Spin States, Obtained from B3PW91 Calculations[a]

method	n[b]	three silver ions	spin state	Ag1−O[c]	Ag2−O[c]	Ag3−O[c]
B3PW91	1	D_{3h}-like cluster	singlet	2.318	2.375	2.377
B3PW91	2	D_{3h}-like cluster	doublet	2.315, 2.399	2.435, 2.466, 2.466	2.391, 2.472
B3PW91	3	isolated ions	singlet	2.335, 2.414, 2.426	2.301, 2.342, 2.379	2.400, 2.372, 2.630

[a] Corresponding values obtained from B3LYP calculations can be seen in Table S4 (Supporting Information). [b] n: number of substituted Al atom inside a ZSM-5 model. [c] Ag−O (Å): Ag−O separations are seen in Figure 2, where atom numberings are also given.

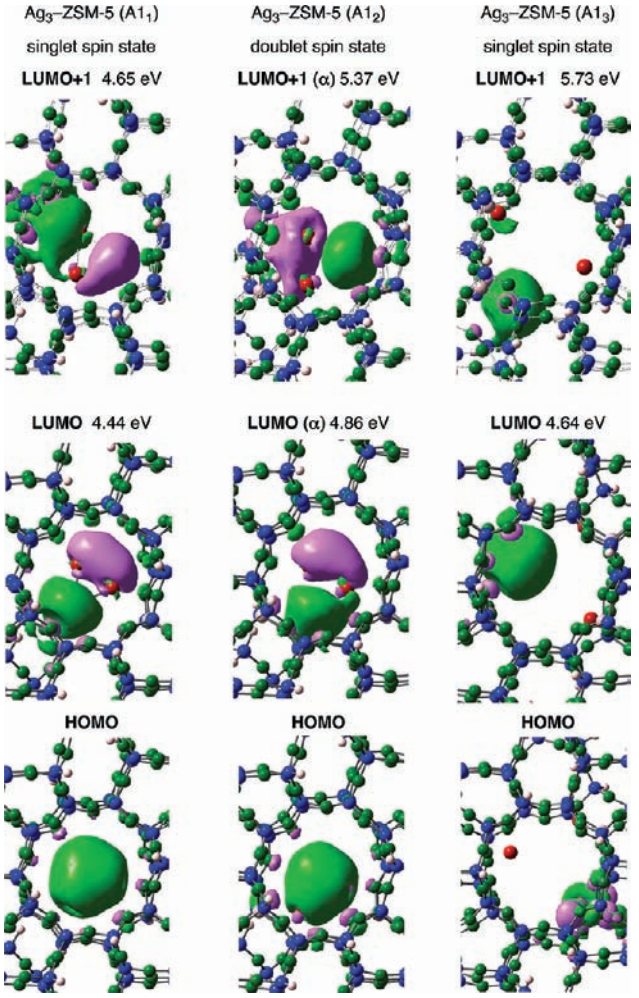

Figure 3. Frontier orbitals of lower spin states of Ag_3−ZSM-5(Al_n) where n varies from 1 to 3. Orbital energies (in eV) of the LUMO and LUMO+1 relative to the HOMO are obtained from the B3PW91 calculations. Corresponding values obtained from B3LYP calculations are seen in ref 58.

information on the optimized Ag−O bond lengths is tabulated in Tables 3 and S4 (Supporting Information). As shown in Figures 2 and S4 (Supporting Information), the behavior of the silver species inside a ZSM-5 cavity follows the electron-count argument. Actually, the structural features of the enclosed Ag_3 species are strongly affected by the number of substituted Al atoms. Figure 2 shows that the silver species inside the ZSM-5(Al_1) and ZSM-5(Al_2) cavities take D_{3h}-like triangle clusters. Ag_3−ZSM-5(Al_1) contains a nearly equilateral triangle whose Ag−Ag separations are around 2.70 Å, while in Ag_3−ZSM-5(Al_2) there is an isosceles triangle slightly distorted from a D_{3h} structure (two Ag−Ag separations around 2.88 Å plus one Ag−Ag separation of

Table 4. Electronic Properties of Ag_3−ZSM-5(Al_n) in Lower Spin States, Obtained from B3PW91 Calculations.[a]

				spin density[c]			NPA charge[d]		
method	n[b]	three silver ions	spin state	Ag1	Ag2	Ag3	Ag1	Ag2	Ag3
B3PW91	1	D_{3h}-like cluster	singlet				0.20	0.17	0.08
B3PW91	2	D_{3h}-like cluster	doublet	0.33	0.21	0.40	0.43	0.49	0.43
B3PW91	3	isolated ions	singlet				0.80	0.66	0.53

[a] Corresponding values obtained from B3LYP calculations can be seen in Table S6 (Supporting Information). [b] n: number of substituted Al atoms inside a ZSM-5 model. [c] Spin density; calculated spin density integrated over atomic basin of an atom. Atom numberings are given in Figure 2. [d] NPA charge; calculated charge density of an atom obtained from natural population analyses (NPA). Detailed information can be seen in Tables S7−S9 (Supporting Information).

2.84 Å). In contrast, such triangle cluster cannot be formed in ZSM-5(Al_3) zeolite; three silver atoms separate each other by 5.56−6.98 Å at the B3PW91 calculation. Instead, each silver cation is bound to two or three framework oxygen atoms, being similar to the Ag_1−ZSM-5(Al_1) case. Actually, similar Ag−O separations are found in Ag_3−ZSM-5(Al_3) and Ag_1−ZSM-5(Al_1) (Figure S5 (Supporting Information)); their separations range from 2.34 to 2.64 Å in Tables 3 and S5 (Supporting Information). These results suggest that the silver cations in Ag_3−ZSM-5(Al_3) prefer to bind into framework oxygen atoms rather than to aggregate each other. In other words, the Ag−O interactions play more dominant roles in determining the structural features of Ag_3−ZSM-5(Al_3) than the Ag−Ag interactions.

In order to clarify factors in the cluster formation inside a ZSM-5 cavity, we turn to their frontier orbitals in Figure 3. Frontier orbitals of Ag_3−ZSM-5(Al_1) and Ag_3−ZSM-5(Al_2) are made up of their 5s(Ag) orbitals; the HOMOs are totally symmetric, whereas the LUMOs and LUMO+1s have one node. Since the totally symmetric orbitals have in-phase interactions between adjacent silver atoms, the attractive orbital interactions are a major source of forming the triangle clusters. Net NPA charges for the Ag_3 clusters in Ag_3−ZSM-5(Al_1) and Ag_3−ZSM-5(Al_2) are, respectively, 0.45 and 1.35 at the B3PW91 calculations (Table 4). Corresponding NPA values obtained from B3LYP calculations are given in Table S6 (Supporting Information). See detailed information on electronic configurations of Ag_3−ZSM-5(Al_n) in Tables S7−S9 (Supporting Information).

The orbital features of Ag_3−ZSM-5(Al_1) and Ag_3−ZSM-5(Al_2) are analogous to those in Chart 1 in terms of orbital symmetry. Considering the similar orbital symmetry, we expect

dx.doi.org/10.1021/ic2001514 |Inorg. Chem. 2011, 50, 6533–6542

that an electron in the a_1-like HOMO can be excited to the e′-like LUMO or LUMO+1 by photoirradiation from an analogy to the bare Ag_3^+ cases. The HOMO−LUMO gap in Ag_3−ZSM-5(Al_1) is 4.4 eV, and that in Ag_3−ZSM-5(Al_2) is 4.9 eV.[58] The calculated gaps may explain the absorption bands of Ag−ZSM-5 at 255 and 305 nm. The energy levels of the HOMO and LUMO (LUMO+1) are determined by not only Ag−Ag orbital interactions but also Ag−O orbital interactions. Thus, the Ag−O orbital interactions are an important factor in determining absorption band positions of Ag−ZSM-5.

In contrast to the Ag_3−ZSM-5(Al_1) and Ag_3−ZSM-5(Al_2) cases, the summation of the NPA charges for three silver atoms in Ag_3−ZSM-5(Al_3) gives a larger value (1.99 and 1.94 obtained from the B3PW91 and B3LYP calculations, respectively, in Tables 4 and S6 (Supporting Information)). Considering the total NPA charge together with the frontier orbitals of the Ag_3^+ cluster (Chart 1), each silver cation cannot gain substantial attractive interactions with a neighboring cation. Then all cations approach to extraframework oxygen atoms because of the electrostatic attractive interactions. Accordingly, Ag_3−ZSM-5(Al_3) has quite different orbital features in frontier orbital regions; the HOMO exhibits 4d character, whereas the LUMO exhibits 5s character. The electronic properties in Ag_3−ZSM-5(Al_3), such as their frontier orbitals and NPA charges, are basically similar to those in the Ag_1−ZSM-5(Al_1) given in Figure S6 and Table S10 (Supporting Information).

From Figures 2 and 3, the number of substituted Al atoms has a striking influence on the properties of Ag_3−ZSM-5(Al_n); the size of the triangle cluster increases with the number of n. Key factors in determining the structures of three silver cations inside a ZSM-5 cavity can be schematically explained in Chart 4. First, the attractive interactions coming from the totally symmetric orbital of silver ions are a main key in cluster formation. Whether the symmetric orbital is occupied or not is determined by the NPA charges that are directly connected to the number of substituted Al atoms (n). Another important factor is the existence of more oxygen atoms charged negatively in a larger

Chart 4

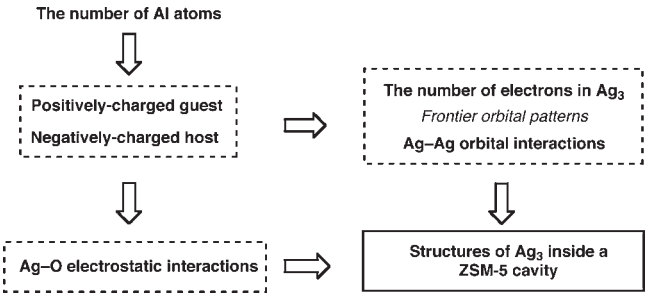

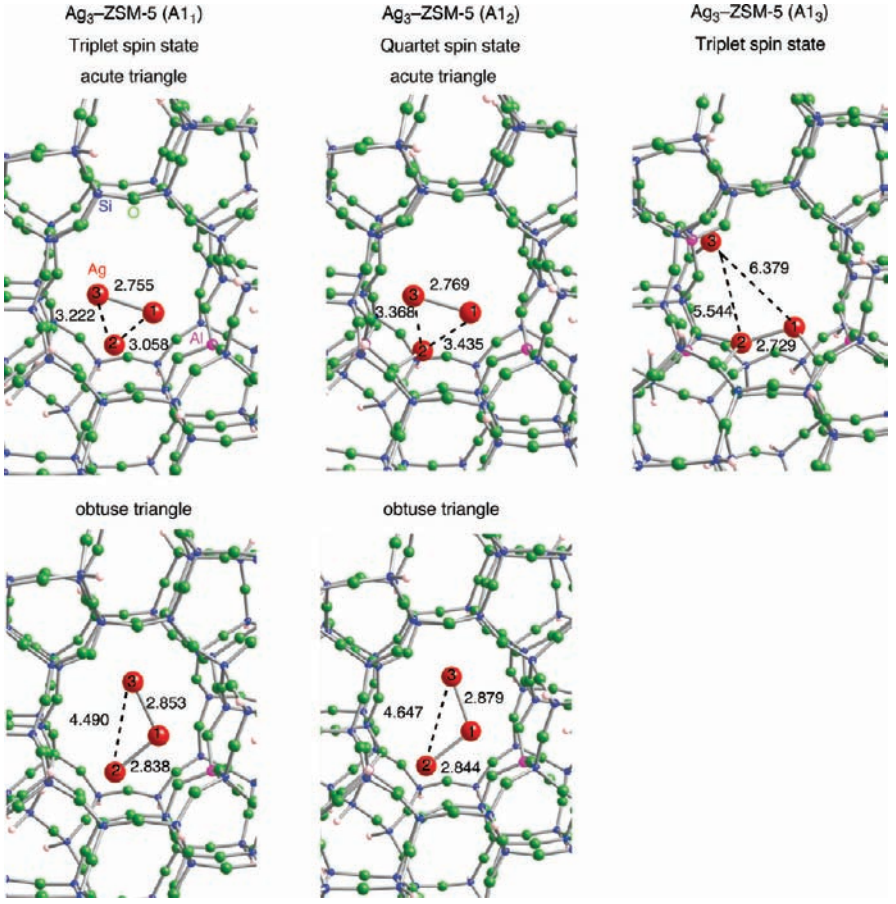

Figure 4. B3PW91-optimized Ag_3−ZSM-5(Al_n) structures in higher spin states where n varies from 1 to 3. Ag_3−ZSM-5(Al_1) and Ag_3−ZSM-5(Al_3) in the triplet spin state and Ag_3−ZSM-5(Al_2) in the quartet spin state are given. The Ag−Ag separations are given in Angstroms. Corresponding B3LYP-optimized geometries are given in Figure S7 (Supporting Information). Details of optimized Ag−O bond lengths can be seen in Tables 5 and S11 (Supporting Information).

dx.doi.org/10.1021/ic2001514 |Inorg. Chem. 2011, 50, 6533–6542

Table 5. Ag−O Bond Lengths of Ag_3−ZSM-5(Al_n) in Higher Spin States, Obtained from B3PW91 Calculations.[a]

method	n[b]	three silver ions	spin state	Ag1−O[c]	Ag2−O[c]	Ag3−O[c]
B3PW91	1	obtuse triangle	triplet	2.402, 2.591	2.661	2.494
B3PW91	1	acute triangle	triplet	2.420, 2.424		2.388
B3PW91	2	obtuse triangle	quartet	2.427, 2.561	2.163, 2.344, 2.391	2.565
B3PW91	2	acute triangle	quartet	2.396, 2.504	2.174, 2.607, 2.349	2.481
B3PW91	3	linear cluster plus one ion	triplet	2.235, 2.405	2.254, 2.254, 2.531	2.284, 2.322, 2.638

[a] Corresponding values obtained from B3LYP calculations can be seen in Table S11 (Supporting Information). [b] n: number of substituted Al atoms inside a ZSM-5 model. [c] Ag−O (Å): Ag−O separations are seen in Figure 4, where atom numberings are also given.

number of Al atoms. In that situation, silver cations have larger coordination numbers, indicating that stronger electrostatic interactions are exerted between three silver ions and a ZSM-5 framework. Consequently, weaker Ag−Ag interactions as well as stronger Ag−O interactions operate in larger n. The DFT results demonstrate that the balance between the Ag−Ag and the Ag−O interactions plays a dominant role in determining the structures of silver species inside a ZSM-5 cavity. Despite the interesting DFT findings, we need further investigation into the Al-position dependences of the Ag_3 clusters inside a ZSM-5 cavity, because substituted Al atoms are randomly distributed within a ZSM-5 framework experimentally.

Properties of Ag_3−ZSM-5 in Higher Spin States. Next, we discuss the Ag_3−ZSM-5 structures in higher spin states depending on the number of substituted Al atoms (n). In the triplet state of Ag_3−ZSM-5(Al_1) and the quartet state of Ag_3−ZSM-5(Al_2), an antisymmetric orbital in Figure 3 is occupied by one electron from the HOMO (symmetric orbital), which is in line with the electron excitation of the bare Ag_3^+ cluster. In the Ag−Ag interactions in the higher spin states, the symmetric orbital as well as an antisymmetric orbital are important. Occupation of an antisymmetric orbital differentiates its higher spin states from lower spin states. Figure 3 shows that the lower spin states have two antisymmetric orbitals (the LUMO and the LUMO+1) lying close in energy. Accordingly, we obtained two types of optimized geometries for higher states of Ag_3−ZSM-5(Al_1) and Ag_3−ZSM-5(Al_2) at B3PW91 calculations (Figure 4). Corresponding B3LYP-optimized geometries are displayed in Figure S7 (Supporting Information). Their key geometrical parameters are shown in Tables 5 and S11 (Supporting Information). Their frontier orbitals are shown in Figures 5 and S8 (Supporting Information). Figure 4 shows that both optimized structures have triangles distorted significantly from D_{3h} symmetry. The existence of two types of distorted triangle in a ZSM-5 cavity (acute and obtuse triangles) is similar to the bare Ag_3^+ case in the triplet state (Figure 1) where Jahn−Teller distortion can be seen. We see from Table 6 that the energy differences between the two triangles do not significantly change by encapsulation into a ZSM-5 cavity.

Despite the similarity in terms of energetics, the distortion of triangle clusters in higher states of Ag_3−ZSM-5(Al_1) and Ag_3−ZSM-5(Al_2) is more pronounced than the bare Ag_3^+ cluster in the triplet state. In the obtuse triangles inside ZSM-5 cavities with single and double substitution, two silver ions are apart by ∼4.50 and ∼4.65 Å, respectively. Accordingly, the optimized angles of ∠Ag2−Ag1−Ag3 are 104.2−108.6°. In contrast, the acute triangles have one silver ion separating them from the other ions. Then we found a smaller ∠Ag1−Ag2−Ag3 around 50° and two enlarged separations (Ag1−Ag2 and Ag2−Ag3) ranging from 3.06 to 3.44 Å in the B3PW91 calculation. These results suggest that the cluster distortion inside a ZSM-5 cavity is significant relative to those in the bare Ag_3^+ cluster in the triplet state owing to bindings of silver species into framework oxygen atoms. The distortion may be important in enhancing the catalytic activity of Ag−ZSM-5, because it generates coordinatively unsaturated silver atoms with a space for guests to approach directly.

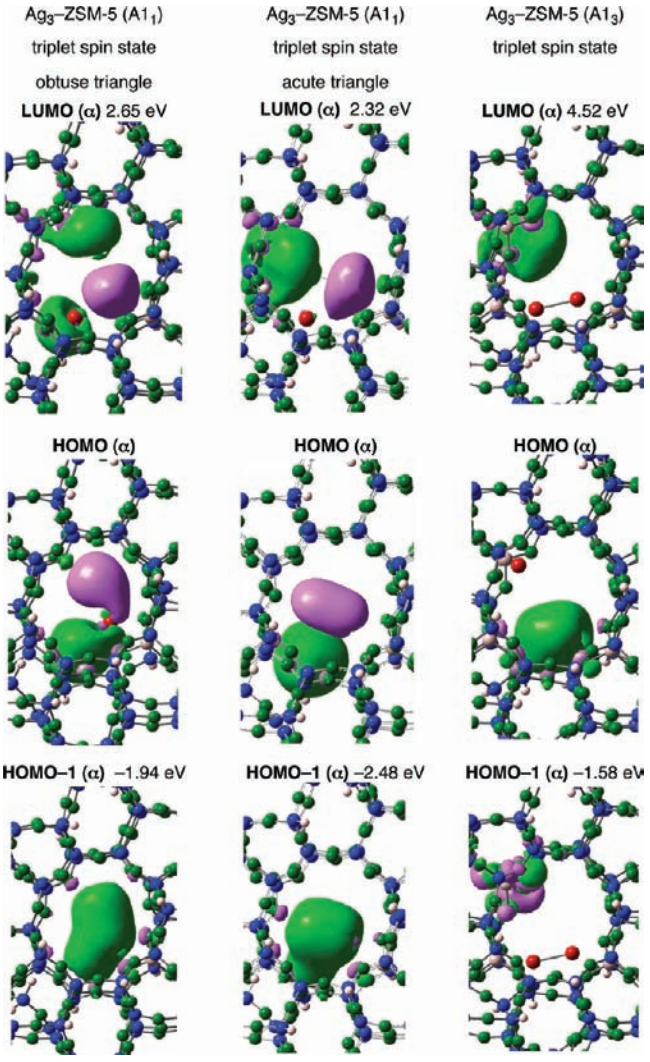

Figure 5. Frontier orbitals of higher spin states of Ag_3−ZSM-5(Al_n) where n is 1 and 3. Orbital energies (in eV) of the LUMO and LUMO+1 relative to the HOMO are obtained from the B3PW91 calculations. Corresponding orbitals of Ag_3−ZSM-5(Al_2) are given in Figure S8 (Supporting Information).

Reflecting from the different geometries of the two enclosed triangles, patterns of the spin density distribution are quite

dx.doi.org/10.1021/ic2001514 |Inorg. Chem. 2011, 50, 6533–6542

Table 6. Electronic Properties of Ag_3−ZSM-5 (Al_n) in Higher Spin States, Obtained from B3PW91 Calculations[a]

				spin density[c]			NPA charge[d]			
method	n[b]	three silver ions	spin state	Ag1	Ag2	Ag3	Ag1	Ag2	Ag3	ΔE[e]
B3PW91	1	obtuse triangle	triplet	0.48	0.72	0.72	0.18	0.17	0.19	0
B3PW91	1	acute triangle	triplet	0.38	0.88	0.67	0.31	0.05	0.16	2.02
B3PW91	2	obtuse triangle	quartet	0.58	1.07	0.74	0.23	0.57	0.21	0.14
B3PW91	2	acute triangle	quartet	0.45	1.47	0.52	0.35	0.42	0.22	0
B3PW91	3	linear cluster plus one ion	triplet	0.70	0.80	0.00	0.55	0.54	0.54	

[a] Corresponding values obtained from B3LYP calculations can be seen in Table S12 (Supporting Information). [b] n: number of substituted Al atoms inside a ZSM-5 model. [c] Spin density; calculated spin density integrated over atomic basin of an atom. Atom numberings are given in Figure 4. [d] NPA charge; calculated charge density of an atom obtained from natural population analyses (NPA). Detailed information can be seen in Tables S7−S9 (Supporting Information). [e] ΔE (kcal/mol): energy of a triangle relative the most stable conformation. When a triangle is the most stable conformation, ΔE is 0.

different, as shown in Tables 6 and S12 (Supporting Information). Roughly speaking, in the enclosed obtuse triangles, the two silver atoms separating each other (Ag2 and Ag3) have significant spin densities, whereas the other silver atom (Ag1) does not. In the enclosed acute triangles, significant spin densities appear at the silver atom (Ag2) that is far from the other two atoms. The spin density distributions are similar to those in the bare Ag_3^+ cluster in higher spin states. The patterns of the spin density distribution are understandable from their singly occupied molecular orbitals (SOMOs), whose orbital amplitudes are found in Figure 5. Unpaired electrons exist in symmetric and antisymmetric orbitals in the higher spin states which can be generated by photoirradiation. Since radical Ag cations can have the power to cleave a C−H bond of hydrocarbons in a homolytic manner, the silver cations inside a ZSM-5 cavity may become reactive toward hydrocarbons under photoirradiation. Despite the similarity in spin distributions of the Ag_3 cluster with and without the ZSM-5 surroundings, there is a slight difference in the spin density distributions; spin densities of silver cations near the Al substitution are less than those in the bare cluster. The slight discrepancy in the spin density distributions may give us a hint to elucidate Al positions within a 10-membered ring of ZSM-5.

Although we found more significant Ag_3 distortion inside ZSM-5(Al_1) and ZSM-5(Al_2) by changing from the lower states to the higher states, the ZSM-5(Al_3) case has opposite trends between the two states. In fact, Figure 4 shows that the triplet spin state of Ag_3−ZSM-5(Al_3) has two silver cations approaching by ∼2.73 Å, different from its singlet state where three ions are isolated. Formation of the linear cluster in the triplet state can be understood by the HOMO where a 5s orbital interacts with a 5s orbital in a bonding fashion (Figure 5). Occupation of the 5s orbitals in Ag_3−ZSM-5(Al_3) is characteristic in the triplet state, which cannot be seen in the singlet state where each 5s orbital is unoccupied. A similar relationship can be seen in the singlet and triplet states of Ag_1−ZSM-5(Al_1) (Figure S6 (Supporting Information)). Owing to a SOMO orbital with two 5s orbitals interacting in an in-phase manner, the linear structure has radical character at both atoms, indicating different reactivity in Ag_3−ZSM-5(Al_3) compared with those in Ag_3−ZSM-5(Al_1) and Ag_3−ZSM-5(Al_2).

CONCLUSIONS

The behavior of Ag_3 clusters inside a nanometer-size cavity of ZSM-5 zeolite with a different number of substituted Al atoms (ZSM-5(Al_n); $1 \le n \le 3$) was investigated by means of density functional theory (DFT) calculations. Comparison in the Ag_3 clusters with and without ZSM surroundings provides the basis to clarify factors determining their structures inside its cavity. DFT calculations demonstrate that Ag−Ag orbital interactions as well as Ag−O electrostatic interactions govern whether an enclosed triangle Ag_3 cluster can be generated in lower and higher spin states of Ag_3−ZSM-5(Al_n). Then the number of substituted Al atoms can control the strength of both interactions; stronger Ag−Ag interactions and weaker Ag−O interactions operate with a smaller number of Al atoms. In the lower spin states, the Ag−Ag interactions come from the totally symmetric orbital consisting of three 5s(Ag) orbitals. Inside ZSM-5 cavities with single and double Al substitutions, D_{3h}-like Ag_3 triangles are contained, whereas three silver ions are isolated in triplet substitution. The cluster structures in lower spin states of Ag_3−ZSM-5(Al_1) and Ag_3−ZSM-5(Al_2) are analogous from the bare Ag_3^+ cluster with the $(a_1)^2(e')^0$ configuration. In contrast, higher spin states of Ag_3−ZSM-5(Al_1) and Ag_3−ZSM-5(Al_2) have two types of triangles significantly distorted from the D_{3h} structure, whereas a linear Ag_2 cluster is formed in a higher spin state of Ag_3−ZSM-5(Al_3). In the qualitative interpretations of the distorted triangles of Ag_3−ZSM-5(Al_1) and Ag_3−ZSM-5(Al_2), analogies to Jahn−Teller distortion in the bare Ag_3^+ cluster in the triplet state are helpful. In other words, two orbitals with one node are responsible for the existence of two types of distorted Ag_3 cluster in their higher spin states. Furthermore, bindings of an Ag_3 cluster into framework oxygen atoms facilitate significant distortion. Consequently, the DFT calculations found that the structural and electronic features of the enclosed silver clusters are governed by the number of Al atoms through the Ag−Ag and Ag−O interactions. The DFT findings are helpful to understand the catalytic activity of Ag−ZSM-5.

ASSOCIATED CONTENT

Supporting Information. Searching DFT functional suitable to describe the bare Ag_3 cluster, Jahn−Teller distortion of the Ag_3^+ cluster in the triplet spin state, and properties of Ag_1−ZSM-5(Al_1). ZSM-5 modeling (Figure S1); optimized structures for bare Ag_3 clusters (Figure S2); Jahn−Teller distortion of the bare Ag_3^+ cluster in the singlet and triplet states in the B3LYP calculations (Figure S3); optimized Ag_3−ZSM-5(Al_n) structures in lower spin states obtained from B3LYP calculations (Figure S4); optimized structures for Ag_1−ZSM-5(Al_1) in the

dx.doi.org/10.1021/ic2001514 |Inorg. Chem. 2011, 50, 6533–6542

singlet and triplet spin states (Figure S5); frontier orbitals of $Ag_1-ZSM\text{-}5(Al_1)$ in the singlet and triplet spin states (Figure S6); optimized $Ag_3-ZSM\text{-}5(Al_n)$ structures in higher spin states obtained from the B3LYP calculations (Figure S7); frontier orbitals of $Ag_3-ZSM\text{-}5(Al_2)$ in the quartet spin state (Figure S8); key parameters of bare Ag_3 clusters (Table S1); dependences of the structures of the singlet Ag_3^+ cluster on calculation methods (B3PW91, B3LYP, PBEPBE, and CCSD methods) (Table S2); key parameters of bare Ag_3^+ clusters in the triplet spin states obtained from B3LYP and PBEPBE calculations (Table S3); Ag−O bond lengths of B3LYP-optimized $Ag_3-ZSM\text{-}5(Al_n)$ structures in lower spin states (Table S4); key parameters of $Ag_1-ZSM\text{-}5(Al_1)$ (Table S5); electronic properties of $Ag_3-ZSM\text{-}5(Al_n)$ in lower spin states obtained from B3LYP calculations (Table S6); electronic configurations of $Ag_3-ZSM\text{-}5(Al_1)$ based on NPA (Table S7); electronic configurations of $Ag_3-ZSM\text{-}5(Al_2)$ based on NPA (Table S8); electronic configurations of $Ag_3-ZSM\text{-}5(Al_3)$ based on NPA (Table S9); electronic configurations of $Ag_1-ZSM\text{-}5(Al_1)$ based on natural atomic orbital analyses (NPA) (Table S10); Ag−O bond lengths of B3LYP-optimized $Ag_3-ZSM\text{-}5(Al_n)$ structures in higher spin states (Table S11); electronic properties of $Ag_3-ZSM\text{-}5(Al_n)$ in lower spin states obtained from B3LYP calculations (Table S12). This material is available free of charge via the Internet at http://pubs.acs.org.

AUTHOR INFORMATION

Corresponding Author
*E-mail: yumura@chem.kit.ac.jp.

ACKNOWLEDGMENT

The authors thank Prof. Petr. Nachtigall at Charles University (Czech Republic) for valuable discussion on the behavior of silver species inside a ZSM-5 cavity. The project was partially supported by a Grant-in-Aid for Young Scientists (B) from the Japan Society for the Promotion of Science (JSPS) (T.Y. at Kyoto Institute of Technology) (No. 22710088). At Okayama University, financial support was provided by the Ministry of Education, Culture, Sports, Science, and Technology of Japan (Nos. 17034046, 17655061, 17036043, 18033037, and 21655021). H.T. acknowledges the financial support for Young Scientists (DC1) from JSPS.

REFERENCES

(1) Baelocher, Ch.; Meier, W. M.; Olson, D. H. *Atlas of Zeolite Framework Types*, 5th ed.; Elsevier: Amsterdam, 2001.
(2) Shelef, M. *Chem. Rev.* **1995**, *95*, 209.
(3) Corma, A. *Chem. Rev.* **1995**, *95*, 559.
(4) van Santen, R. A.; Kramer, G. J. *Chem. Rev.* **1995**, *95*, 637.
(5) Huheey, J. E. *Inorganic Chemistry*, Xth ed.; Harper & Row: New York.
(6) Schriver, D. F.; Atkins, P. W. *Inorganic Chemistry*, 4th ed.; Oxford University Press: Oxford, 2006.
(7) Iijima, S. *Nature* **1991**, *354*, 56.
(8) Iijima, S.; Ichihashi, T. *Nature* **1993**, *363*, 603.
(9) Smith, B. W.; Monthioux, M.; Luzzi, D. E. *Nature* **1998**, *396*, 323.
(10) Khobystov, A. N.; Britz, D. A.; Briggs, G. A. D. *Acc. Chem. Res.* **2005**, *38*, 901.
(11) Yumura, T.; Takeuchi, M.; Kobayashi, H.; Kuroda, Y. *Inorg. Chem.* **2009**, *48*, 508.
(12) (a) Yumura, T.; Kertesz, M.; Iijima, S. *J. Phys. Chem. B* **2007**, *111*, 1099. (b) Yumura, T.; Kertesz, M. *Chem. Mater.* **2007**, *19*, 1028. (c) Yumura, T.; Kertesz, M.; Iijima, S. *Chem. Phys. Lett.* **2007**, *444*, 155. (d) Yumura, T. *Phys. Chem. Chem. Phys.* **2011**, *13*, 337.
(13) (a) Beyer, H.; Jacobs, P. A.; Uytterhoeven, J. B. *J. Chem. Soc., Faraday Trans. I* **1976**, *72*, 674. (b) Jacobs, P. A.; Uytterhoeven, J. B.; Beyer, K. H. *J. Chem. Soc., Faraday Trans. I* **1977**, *73*, 1755. (c) Jacobs, P. A.; Uytterhoeven, J. B.; Beyer, K. H. *J. Chem. Soc., Faraday Trans. I* **1979**, *75*, 56.
(14) (a) Kim, Y.; Seff, K. *J. Am. Chem. Soc.* **1978**, *100*, 6989. (b) Sun, T.; Seff, K. *Chem. Rev.* **1994**, *94*, 857. (c) Kim, S. Y.; Kim, Y.; Seff, K. *J. Phys. Chem. B* **2003**, *107*, 6938.
(15) (a) Gellens, L. R.; Mortier, W. J.; Schoonheydt, R. A.; Uytterhoeven, J. B. *J. Phys. Chem.* **1981**, *85*, 2783. (b) Schoonheydt, R. A.; Leeman, H. *J. Phys. Chem.* **1989**, *93*, 2048.
(16) (a) Ozin, G. A.; Hugues, F. *J. Phys. Chem.* **1982**, *86*, 5174. (b) Ozin, G. A.; Hugues, F. *J. Phys. Chem.* **1983**, *87*, 94. (c) Ozin, G. A.; Hugues, F.; Mattar, S. M.; McIntosh, D. F. *J. Phys. Chem.* **1983**, *87*, 3445. (d) Baker, M. D.; Ozin, G. A.; Godber, J. *J. Phys. Chem.* **1984**, *88*, 4902. (e) Baker, M. D.; Ozin, G. A.; Godber, J. *J. Phys. Chem.* **1985**, *89*, 305.
(17) (a) Brown, D. R.; Kevan, L. *J. Phys. Chem.* **1986**, *90*, 1129. (b) Xu, B.; Kevan, L. *J. Phys. Chem.* **1991**, *95*, 1147.
(18) Texter, J.; Kellerman, R.; Gonsiorowski, T. *J. Phys. Chem.* **1986**, *90*, 2118.
(19) Gachard, E.; Belloni, J.; Subramanian, M. A. *J. Mater. Chem.* **1996**, *6*, 867.
(20) (a) Anpo, M.; Matsuoka, M.; Yamashita, H. *Catal. Today* **1997**, *35*, 177. (b) Anpo, M.; Zhang, S. G.; Mishima, H.; Matsuoka, M.; Yamashita, H. *Catal. Today* **1997**, *39*, 159. (c) Kanan, S. M.; Omary, M. A.; Patterson, H. H.; Matsuoka, M.; Anpo, M. *J. Phys. Chem. B* **2000**, *104*, 3507. (d) Ju, W.-S.; Matsuoka, M.; Iino, K.; Yamashita, H.; Anpo, M. *J. Phys. Chem. B* **2004**, *108*, 2128.
(21) Kanan, S. M.; Kanan, M. C.; Patterson, H. H. *J. Phys. Chem. B* **2001**, *105*, 7508.
(22) (a) Shibata, J.; Shimizu, K.; Takada, Y.; Shichi, A.; Yoshida, H.; Satokawa, S.; Satsuma, A.; Hattori, T. *J. Catal.* **2004**, *227*, 367. (b) Shimizu, K.; Sugino, K.; Kato, K.; Yokota, S.; Okumura, K.; Satsuma, A. *J. Phys. Chem. C* **2007**, *111*, 1683. (c) Sawabe, K.; Hiro, T.; Shimizu, K.; Satsuma, A. *Catal. Today* **2010**, *153*, 90.
(23) (a) Baba, T.; Komatsu, N.; Sawada, H.; Yamaguchi, Y.; Takahashi, T.; Sugisawa, H.; Ono, Y. *Langmuir* **1999**, *15*, 7894. (b) Baba, T.; Sawada, H. *Phys. Chem. Chem. Phys.* **2002**, *4*, 3919. (c) Baba, T.; Sawada, H.; Takahashi, T.; Abe, M. *Appl. Catal., A* **2002**, *231*, 55.
(24) Yoshida, H.; Hamajima, T.; Kato, Y.; Shibata, J.; Satsuma, A.; Hattori, T. *Res. Chem. Intermed.* **2003**, *29*, 897.
(25) Miao, S.; Wang, Y.; Ma, D.; Zhu, Q.; Zhou, S.; Su, L.; Tan, D.; Bao, X. *J. Phys. Chem. B* **2004**, *108*, 17866.
(26) (a) Cremer, G. D.; Antoku, Y.; Roeffaers, M. B. J.; Sliwa, M.; Noyen, J. V.; Smout, S.; Hofkens, J.; Vos, D. E. D.; Sels, B. F.; Vosch, T. *Angew. Chem., Int. Ed.* **2008**, *47*, 2813. (b) Cremer, G. D.; Coutino-Gonzalez, E.; Roeffaers, M. B. J.; Moens, B.; Ollevier, J.; Auweraer, M. V. d.; Schoonheydt, R.; Jacobs, P. A.; Schryver, F. C. D.; Hofkens, J.; Vos, D. E. D.; Sels, B. F.; Vosch, T. *J. Am. Chem. Soc.* **2009**, *131*, 3049. (c) Cremer, G. D.; Sels, B. F.; Hotta, J.; Roeffaers, M. B. J.; Bartholomeeusen, E.; Coutino-Gonzalez, E.; Valtchev, V.; Vos, D. E. D.; Vosch, T.; Hofkens, J. *Adv. Mater.* **2010**, *22*, 957. (d) De Cremer, G.; Coutiño-Gonzalez, E.; Roeffaers, M. B. J.; De Vos, D. E.; Hofkens, J.; Vosch, T.; Sels, B. F. *ChemPhysChem* **2010**, *11*, 1627. (e) Royon, A.; Bourhis, K.; Bellec, M.; Papon, G.; Bousquet, B.; Deshayes, Y.; Cardinal, T.; Canioni, L. *Adv. Mater.* **2010**, *22*, 5282.
(27) Yumura, T.; Hirahara, K.; Bandow, S.; Yoshizawa, K.; Iijima, S. *Chem. Phys. Lett.* **2004**, *386*, 38. (b) Yumura, T.; Bandow, S.; Yoshizawa, K.; Iijima, S. *J. Phys. Chem. B* **2004**, *108*, 11426. (c) Yumura, T.; Nozaki, D.; Bandow, S.; Yoshizawa, K.; Iijima, S. *J. Am. Chem. Soc.* **2005**, *127*, 11769.
(28) Haruta, M. *Catal. Today* **1997**, *36*, 153.
(29) Atkins, P. W. *Physical Chemistry*, 5th ed.; Oxford University Press: Oxford, 1994.

(30) (a) Woertink, J. S.; Smeets, P. J.; Groothaert, M. H.; Vance, M. A.; Sels, B. F.; Schoonheydt, R. A.; Solomon, E. I. *Proc. Natl. Acad. Sci.* **2009**, *106*, 18908. (b) Smeets, P. J.; Hadt, R. G.; Woertink, J. S.; Vanelderen, P.; Schoonheydt, R. A.; Sels, B. F.; Solomon, E. I. *J. Am. Chem. Soc.* **2010**, *132*, 14736. (c) Smeets, P. J.; Woertink, J. S.; Sels, B. F.; Solomon, E. I.; Schoonheydt, R. A. *Inorg. Chem.* **2010**, *49*, 3573. (d) Philippaerts, A.; Paulussen, S.; Turner, S.; Lebedev, O. I.; Tendeloo, G. V.; Poelman, H.; Bulut, M.; De Clippel, F.; Smeets, P. J.; Sels, B. F.; Jacobs, P. *J. Catal.* **2010**, *270*, 172.

(31) (a) Itadani, A.; Sugiyama, H.; Tanaka, M.; Ohkubo, T.; Yumura, T.; Kobayashi, H.; Kuroda, Y. *J. Phys. Chem. C* **2009**, *113*, 7213. (b) Yumura, T.; Yamashita, H.; Torigoe, H.; Kobayashi, H.; Kuroda, Y. *Phys. Chem. Chem. Phys.* **2010**, *12*, 2392. (c) Itadani, A.; Yumura, T.; Ohkubo, T.; Kobayashi, H.; Kuroda, Y. *Phys. Chem. Chem. Phys.* **2010**, *12*, 6455. (d) Torigoe, H.; Mori, T.; Fujie, K.; Ohkubo, T.; Itadani, A.; Gotoh, K.; Ishida, H.; Yamashita, H.; Yumura, T.; Kobayashi, H.; Kuroda, Y. *J. Phys. Chem. Lett.* **2010**, *1*, 2642. (e) Yumura, T.; Hasegawa, S.; Itadani, A.; Kobayashi, H.; Kuroda, Y. *Materials* **2010**, *3*, 2516.

(32) The ZSM-5 structure was taken from the Cerius 2 database. Accerys, Software, Inc.: San Diego.

(33) Yanagisawa, S.; Tsuneda, T.; Hirao, H. *J. Chem. Phys.* **2000**, *112*, 545.

(34) Yoon, J.; Kim, K. S.; Baeck, K. K. *J. Chem. Phys.* **2000**, *112*, 9335.

(35) Fournier, R. *J. Chem. Phys.* **2001**, *115*, 2165.

(36) Lee, H. M.; Ge, M.; Sahu, B. R.; Tarakeshwar, P.; Kim, K. S. *J. Phys. Chem. B* **2003**, *107*, 9994.

(37) Zhao, S.; Li, Z.-H.; Wang, W.-N.; Liu, Z.-P.; Fan, K.-N.; Xie, Y.; Schaefer, H. F., III *J. Chem. Phys.* **2006**, *124*, 184102.

(38) (a) Becke, A. D. *Phys. Rev. A* **1988**, *38*, 3098. (b) Becke, A. D. *J. Chem. Phys.* **1993**, *98*, 5648. (c) Stephens, P. J.; Devlin, F. J.; Chabalowski, C. F.; Frisch, M. J. *J. Phys. Chem.* **1994**, *98*, 11623.

(39) Lee, C.; Yang, W.; Parr, R. G. *Phys. Rev. B* **1988**, *37*, 785.

(40) Vosko, S. H.; Wilk, L.; Nusair, M. *Can. J. Phys.* **1980**, *58*, 1200.

(41) (a) Perdew, J. P.; Chevary, J. A.; Vosko, S. H.; Jackson, K. A.; Pederson, M. R.; Singh, D. J.; Fiolhais, C. *Phys. Rev. B* **1992**, *46*, 6671. (b) Perdew, J. P.; Chevary, J. A.; Vosko, S. H.; Jackson, K. A.; Pederson, M. R.; Singh, D. J.; Fiolhais, C. *Phys. Rev. B* **1993**, *48*, 4978(E).

(42) (a) Perdew, J. P.; Burke, K.; Ernzerhof, M. *Phys. Rev. Lett.* **1996**, *77*, 3865. (b) Perdew, J. P.; Burke, K.; Ernzerhof, M. *Phys. Rev. Lett.* **1997**, *78*, 1396.

(43) Cizek, J. *J. Chem. Phys.* **1966**, *45*, 4256.

(44) Paier, J.; Marsman, M.; Kresse, G. *J. Chem. Phys.* **2007**, *127*, 24103.

(45) (a) Seifert, R.; Kunzmann, A.; Calzaferri, G. *Angew. Chem., Int. Ed.* **1998**, *37*, 1521. (b) Seifert, R.; Rytz, R.; Calzaferri, G. *J. Phys. Chem. A* **2000**, *104*, 7473. (c) Calzaferri, G.; Leiggener, C.; Glaus, S.; Schürch, D.; Kuge, K. *Chem. Soc. Rev.* **2003**, *32*, 29.

(46) Jungsuttiwong, S.; Khongpracha, P.; Troung, T. N.; Limtrakul, J. *Stud. Surf. Sci. Catal.* **2001**, *135*, 2518.

(47) Silhan, M.; Nachtigallová, D.; Nachtigall, P. *Phys. Chem. Chem. Phys.* **2001**, *3*, 4791.

(48) Nguyen, H. G.; Konya, G.; Eyring, E. M.; Hunter, D. B.; Truong., T. N. *J. Phys. Chem. C* **2009**, *113*, 12818.

(49) Frisch, M. J. et al. *Gaussian 03*; Gaussian, Inc.: Pittsburgh, PA, 2003.

(50) Frisch, M. J. et al. *Gaussian 09*; Gaussian, Inc.: Wallingford, CT, 2009.

(51) (a) Stevens, W. J.; Basch, H.; Krauss, M. *J. Chem. Phys.* **1984**, *81*, 6026. (b) Stevens, W. J.; Krauss, M.; Basch, H.; Jasien, P. G. *Can. J. Chem.* **1992**, *70*, 612.

(52) (a) Hehre, W. J.; Ditchfield, R.; Pople, J. A. *J. Chem. Phys.* **1972**, *56*, 2257. (b) Francl, M. M.; Pietro, W. J.; Hehre, W. J.; Binkley, J. S.; Gordon, M. S.; DeFrees, D. J.; Pople, J. A. *J. Chem. Phys.* **1982**, *77*, 3654. (c) Hariharan, P. C.; Pople, J. A. *Theor. Chim. Acta* **1973**, *28*, 213.

(53) (a) Binkley, J. S.; Pople, J. A.; Hehre, W. J. *J. Am. Chem. Soc.* **1980**, *102*, 939. (b) Gordon, M. S.; Binkley, J. S.; Pople, J. A.; Pietro, W. J.; Hehre, W. J. *J. Am. Chem. Soc.* **1982**, *104*, 2797. (c) Pietro, W. J.; Francl, M. M.; Hehre, W. J.; DeFrees, D. J.; Pople, J. A.; Binkley, J. S. *J. Am. Chem. Soc.* **1982**, *104*, 5039. (d) Dobbs, K. D.; Hehre, W. J. *J. Comput. Chem.* **1986**, *7*, 359. (e) Dobbs, K. D.; Hehre, W. J. *J. Comput. Chem.* **1987**, *8*, 861. (f) Dobbs, K. D.; Hehre, W. J. *J. Comput. Chem.* **1987**, *8*, 880.

(54) We also obtained the optimized geometries for bare Ag_3^+ cluster in the singlet spin state by using B3LYP/SDD and B3LYP/LANL2dz. The optimized Ag−Ag separations are 2.731 and 2.753 Å at the B3LYP/SDD and B3LYP/LANL2dz methods, respectively. These values are nearly consistent with those obtained in ref 35.

(55) Albright, T. A.; Burdet, J. K.; Whangbo, M.-H. *Orbital Interactions in Chemistry*; John Wiley & Sons, Inc.: New York, 1985.

(56) Jahn, H. A.; Teller, E. *Proc. R. Soc. London* 1937, *A161*, 220.

(57) Yoshizawa, K.; Kato, T.; Yamabe, T. *J. Chem. Phys.* **1998**, *108*, 7637.

(58) Similar HOMO−LUMO gaps were obtained from the B3LYP calculations; the gap in the singlet spin state of Ag_3−ZSM-5(Al_1) is 4.3 eV, and that in the double spin state of Ag_3−ZSM-5(Al_2) is 4.6 eV.